Primary tracheal hyalinizing clear cell carcinoma with EWSR1 rearrangement: A case report

ZHENG WANG[1*], WENKANG ZONG[2*], GUOZHENG GAO[2], XIKE LU[1] and DAQIANG SUN[1]

[1]Department of Thoracic Surgery, Tianjin Chest Hospital Affiliated to Tianjin University, Tianjin 300222, P.R. China; [2]Department of Pathology, Tianjin Chest Hospital Affiliated to Tianjin University, Tianjin 300222, P.R. China

Received September 5, 2024; Accepted November 27, 2024

DOI: 10.3892/ol.2024.14853

Abstract. Hyalinizing clear cell carcinoma (HCCC) is a rare, low-grade epithelial tumor predominantly found in the salivary glands, with tracheal involvement being particularly uncommon. The present study details a case of primary tracheal HCCC and its clinical presentation, diagnostic challenges and the therapeutic approach used. A 34-year-old female patient presented with a 1-month history of intermittent dyspnea. Enhanced chest computed tomography demonstrated a hypervascular nodule occupying two-thirds of the tracheal lumen. Bronchoscopy results showed a mass with significant luminal obstruction. The initial biopsy revealed a poorly differentiated squamous cell carcinoma. The patient underwent surgical resection via a median sternotomy. Histopathology results showed a tumor characterized by trabecular, cord-like and nest-like arrangements within a hyalinized stroma. Immunohistochemistry was positive for carcinoembryonic antigen, cytokeratin (CK)7, CK5/6, pan-CK, epithelial membrane antigen, p40, p63 and p53, with a low Ki-67 index. Fluorescence *in situ* hybridization analysis confirmed Ewing sarcoma RNA binding protein 1 gene rearrangement, leading to a definitive diagnosis of tracheal HCCC. Primary tracheal HCCC is a particularly rare neoplasm with distinct pathological features. The present case highlights the importance of considering HCCC in the differential diagnosis of tracheal tumors, and emphasizes the critical role of comprehensive histopathological and molecular analysis in achieving an accurate diagnosis and guiding treatment.

Correspondence to: Professor Daqiang Sun, Department of Thoracic Surgery, Tianjin Chest Hospital Affiliated to Tianjin University, 261 Taierzhuang South Road, Jinnan, Tianjin 300350, P.R. China
E-mail: sdqmdsr@163.com

*Contributed equally

Key words: hyalinizing clear cell carcinoma, tracheal tumor, EWSR1 gene rearrangement

Introduction

Hyalinizing clear cell carcinoma (HCCC) is a rare, low-grade malignant epithelial tumor predominantly arising in the salivary glands, with occurrences in the lungs being particularly uncommon. The 2021 World Health Organization classification of thoracic tumors first identified HCCC as a distinct pulmonary epithelial neoplasm, characterized by clear and eosinophilic cells arranged in trabecular, nest-like or cord-like patterns within a mucinous and hyalinized stroma. The International Classification of Diseases for Oncology code for HCCC is 8310/31 (1).

The incidence of pulmonary HCCC is low, with ~20 cases reported worldwide. HCCC typically originates from minor salivary glands in the tracheobronchial submucosa, leading to bronchial obstruction, coughing and dyspnea, with hemoptysis being a less common side effect (2). Tracheal HCCC is particularly rare, and to the best of our knowledge, only three cases have been documented in the literature, all in women aged 46-66 years. Of these cases, two were managed surgically (2,3), while one was treated with an endoscopic laser and cryotherapy (4).

The present study reports the case of a 34-year-old female patient who presented with HCCC of the trachea. The initial symptoms included a persistent cough and dyspnea, which were subsequently managed with surgical resection. The present case highlights the diagnostic and therapeutic challenges posed by this rare type of tumor and aims to enhance the understanding of its unique clinical features.

Case report

In February 2021, a 34-year-old woman was referred to Tianjin Chest Hospital Affiliated to Tianjin University (Tianjin, China) with a 1-month history of a persistent cough and intermittent dyspnea, without sputum production, fatigue or chest discomfort. The physical examination was unremarkable, showing a normal thoracic structure with clear breath sounds bilaterally.

Enhanced chest computed tomography (CT) scan results showed a hypervascular nodule, measuring 2.3x2.0 cm, on the posterior wall of the trachea at the level of the thoracic inlet, with no evidence of metastasis to the regional lymph nodes. The lesion occupied approximately two-thirds of the tracheal lumen and was classified as cT2N0M0 based on the

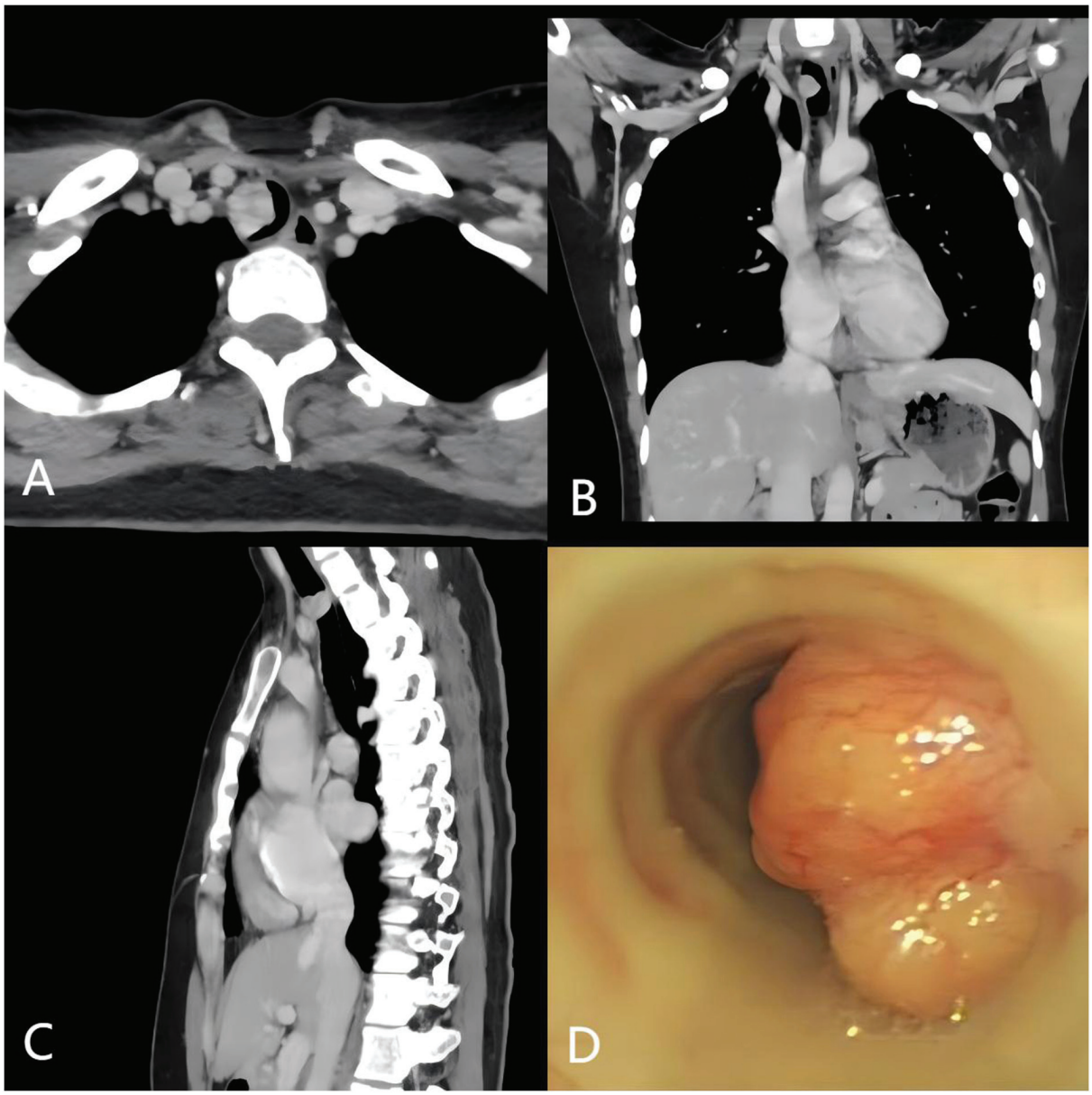

Figure 1. Imaging and bronchoscopic findings of the tracheal tumor. (A) Axial CT scan showing a hypervascular nodule on the posterior wall of the trachea at the level of the thoracic inlet, occupying approximately two-thirds of the tracheal lumen. (B) Coronal CT image demonstrating the vertical extent of the tracheal tumor. (C) Sagittal CT image providing a lateral view of the tumor. (D) Bronchoscopic image revealing a polypoid mass with a broad base and lobulated surface, significantly obstructing the tracheal lumen. CT, computed tomography.

8th edition of the TNM staging system established by the Union for International Cancer Control and the American Joint Committee on Cancer (5). The patient's lactate dehydrogenase (LDH) level was 186 U/l, which was within the normal range (120-250 U/l). Although elevated LDH levels can be associated with tumor presence, the patient's LDH value remained normal, suggesting that LDH may not always be indicative of malignancy in such cases (6). Routine blood count and biochemical analyses were also within normal ranges. The patient reported no personal or family history of tumor-related genetic disorders. Evidence of right-sided tracheal wall invasion raised concerns for possible transmural extension. Subsequent bronchoscopy results showed a broad-based, lobulated mass within the trachea, seven cartilage rings below the glottis, causing significant luminal obstruction (Fig. 1).

A preoperative biopsy suggested poorly differentiated squamous cell carcinoma based on histological and immunohistochemical findings. Histologically, small round tumor cells were observed infiltrating the submucosa, arranged in trabecular or nest-like patterns within fibrous connective tissue. Tumor cells exhibited mild nuclear atypia, uniform size and occasional clear cytoplasm, with no significant keratinization or mitotic figures observed (Fig. 2A and B). Immunohistochemical staining revealed diffuse strong positivity for p40 and p63 (Fig. 2C and D), while markers such as CD56, TTF-1, Napsin A, and Synaptophysin were negative, supporting squamous differentiation. CEA showed partial positivity, while Ki-67 demonstrated a low proliferative index (<10%), and weak positivity for p53 was noted. Based on these findings and the biopsy limitations, an initial diagnosis suggesting poorly differentiated squamous

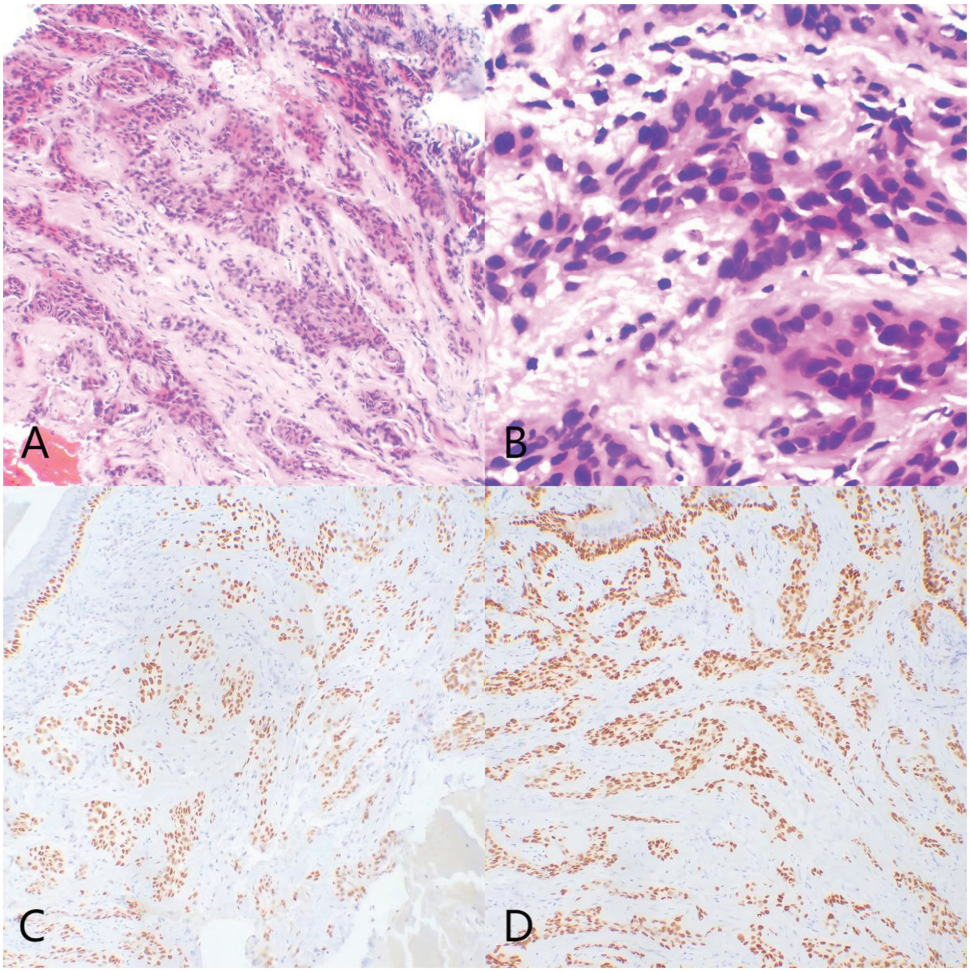

Figure 2. Histopathological and immunohistochemical findings from the preoperative biopsy. (A) H&E staining at low magnification (x100 magnification) showing small round tumor cells infiltrating the fibrous connective tissue, arranged in trabecular and nest-like patterns. (B) H&E staining at high magnification (x400 magnification) highlighting tumor cells with mild nuclear atypia, uniform size and occasional clear cytoplasm, without significant keratinization or mitotic figures. (C) Immunohistochemical staining for p40 at low magnification (x100 magnification), showing diffuse strong positivity in tumor cells. (D) Immunohistochemical staining for p63 at low magnification (x100 magnification), also showing diffuse strong positivity in tumor cells. H&E, hematoxylin and eosin.

cell carcinoma was made, with final confirmation deferred to the surgical resection specimen. In February 2021, the patient underwent a median sternotomy with resection of the tracheal tumor and an end-to-end tracheal anastomosis, all under general anesthesia. The tumor measured ~2x1.5x1 cm and was firm in consistency. Surgical dissection achieved a 1-cm margin on both the superior and inferior edges of the tumor, which was resected using electrocauterization. The primary technical challenges included the proximity of the tumor to critical vascular structures, such as the brachiocephalic artery and common carotid artery, necessitating meticulous dissection to avoid injury to these vessels and the recurrent laryngeal nerve. Additionally, the occupation of the tumor in the tracheal lumen complicated intraoperative airway management. A staged distal tracheal intubation technique was employed to maintain airway patency and oxygenation during tumor resection and tracheal reconstruction. Continuous suturing ensured a watertight anastomosis, minimizing the risk of postoperative airway stenosis or fistula formation. Care was taken to preserve the recurrent laryngeal nerve, preventing postoperative vocal cord dysfunction.

The pathological examination showed a 4.2-cm segment of resected trachea with a proximal and distal circumference of 2.5 and 2.0 cm, respectively. A polypoid, gray-yellow mass measuring 1.7x1.2x1.2 cm protruded into the lumen. Histologically, the tumor was in the submucosa and consisted of cells arranged in trabecular, cord-like and nest-like patterns within a hyalinized stroma. The tumor cells were round to oval and uniform in size, with well-defined cell membranes, mild atypia, clear to eosinophilic cytoplasm, regular nuclear membranes, inconspicuous nucleoli and rare mitotic figures. A number of cells formed glandular structures with mucin secretion, and no keratinization was observed. Mucinous degeneration was noted in areas of the stroma. Tumor tissues were fixed in 10% neutral buffered formalin at room temperature for 24 h, embedded in paraffin, and sectioned at a thickness of 4 μm. Sections were stained with hematoxylin and eosin at room temperature (hematoxylin for 5 min and eosin for 2 min). The histological features were observed under a Leica light microscope (DM3000) with magnifications of x100, x200 and x400 (Fig. 3). Immunohistochemical analysis demonstrated specific marker profiles as follows: Diffuse strong positivity for carcinoembryonic antigen

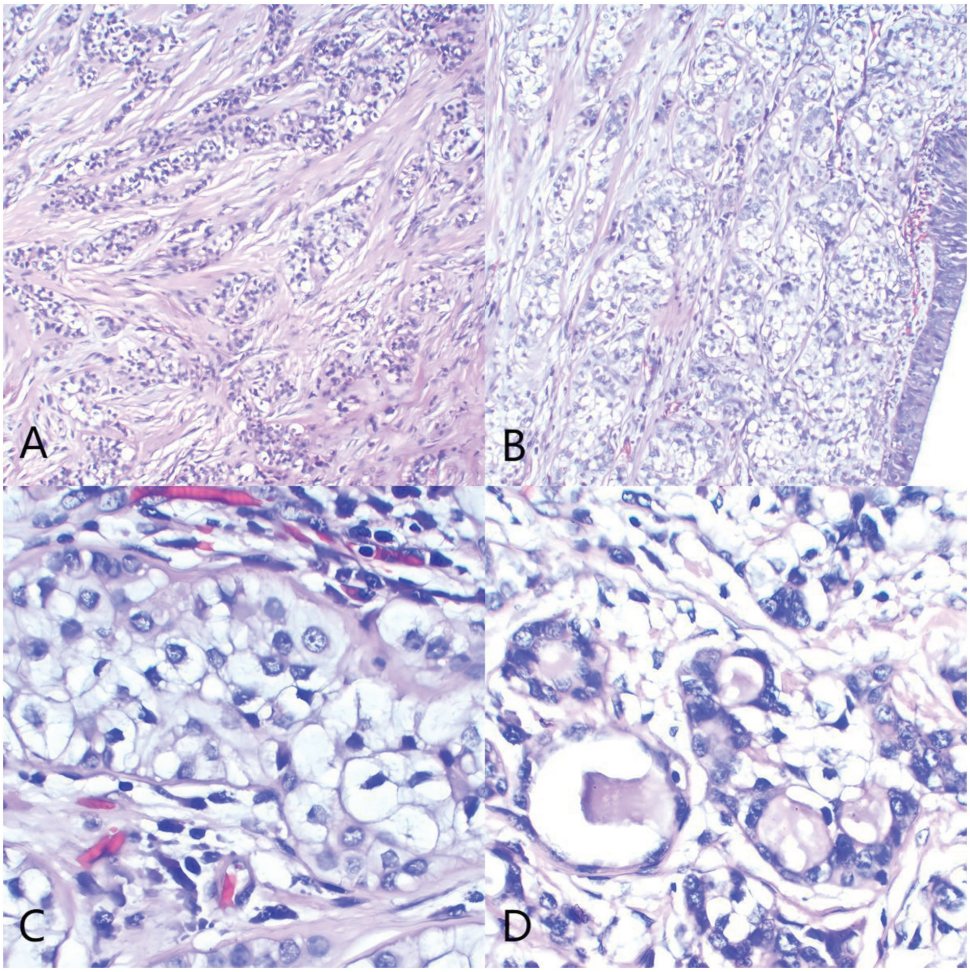

Figure 3. Histopathological characteristics of the tracheal tumor (hematoxylin and eosin staining). (A) Low-power view showing tumor cells embedded in a hyalinized stroma, with clear to eosinophilic cytoplasm (x100 magnification). (B) High-power view highlighting the clear cytoplasm of tumor cells within a hyalinized stroma (x400 magnification). (C) Tumor cells demonstrating mild nuclear atypia, with occasional nucleoli, arranged in trabecular and nest-like patterns (x200 magnification). (D) Glandular structures within the tumor, with mucin secretion visible in the glandular structures (x200 magnification).

(CEA), cytokeratin (CK)7, CK5/6, pan-CK and epithelial membrane antigen, diffuse positivity for p40 and p63, and focal positivity for p53. Tissue sections were blocked with 5% normal goat serum (Beyotime Institute of Biotechnology) at room temperature for 30 min. Primary antibodies, including CEA (dilution 1:200; cat. no. ZM-0096; ZSGB-Bio), CK7 (dilution 1:200; cat. no. ab92742; Abcam), CK5/6 (dilution 1:200; cat. no. ab52635; Abcam), pan-CK (dilution 1:300; cat. no. ZM-0069; ZSGB-Bio), EMA (dilution 1:200; cat. no. ab124964; Abcam), p40 (dilution 1:200; cat. no. ab235897; Abcam), p63 (dilution 1:200; cat. no. ab735; Abcam), Ki-67 (dilution 1:200; cat. no. ab16667; Abcam) and p53 (dilution 1:200; cat. no. ab26; Abcam), were incubated at 4˚C overnight. Secondary antibody (HRP-conjugated anti-rabbit IgG; dilution 1:500; cat. no. 111-035-003; Jackson ImmunoResearch) was incubated at room temperature for 30 min. Chromogen detection was performed using the DAB kit (ZSGB-Bio) following the manufacturer's protocol. The Ki-67 proliferative index was low, at <5% (Fig. 4).

Fluorescence *in situ* hybridization (FISH) was performed on formalin-fixed, paraffin-embedded tissue sections (4-μm thickness). Sections were deparaffinized in xylene, rehydrated in graded ethanol and subjected to proteolytic digestion using pepsin solution (cat. no. P7000; MilliporeSigma) at 37˚C for 15 min. Hybridization was conducted overnight at 37˚C with a dual-color break-apart probe targeting the Ewing sarcoma RNA binding protein 1 (EWSR1; ZytoLight® 22q12.2; ZytoVision) using the ZytoLight FISH-Tissue Implementation Kit (ZytoVision) according to the manufacturer's protocol. Post-hybridization washing was carried out in 0.4X SSC at 72˚C for 2 min, followed by 2X SSC at room temperature for 2 min. FISH signals were visualized using a Leica DM6 B fluorescence microscope (Leica Microsystems) equipped with a DAPI filter at x1,000 magnification. Images were captured and analyzed using CytoVision software (version 7.6; Leica Microsystems). The dual-color break-apart probe consists of fluorescently labeled regions flanking the EWSR1 breakpoint, allowing rearrangements to be identified by the separation of red and green signals. EWSR1 rearrangement was identified in the analyzed sample through FISH (Fig. 5). The final pathological diagnosis was HCCC of the trachea, with full-thickness tracheal wall invasion. The surgical margins were negative for tumor invasion.

The patient was monitored with regular follow-up visits, including chest CT scans, every 3 months. At the most recent follow-up in June 2024, which was 3 years post-surgery, there

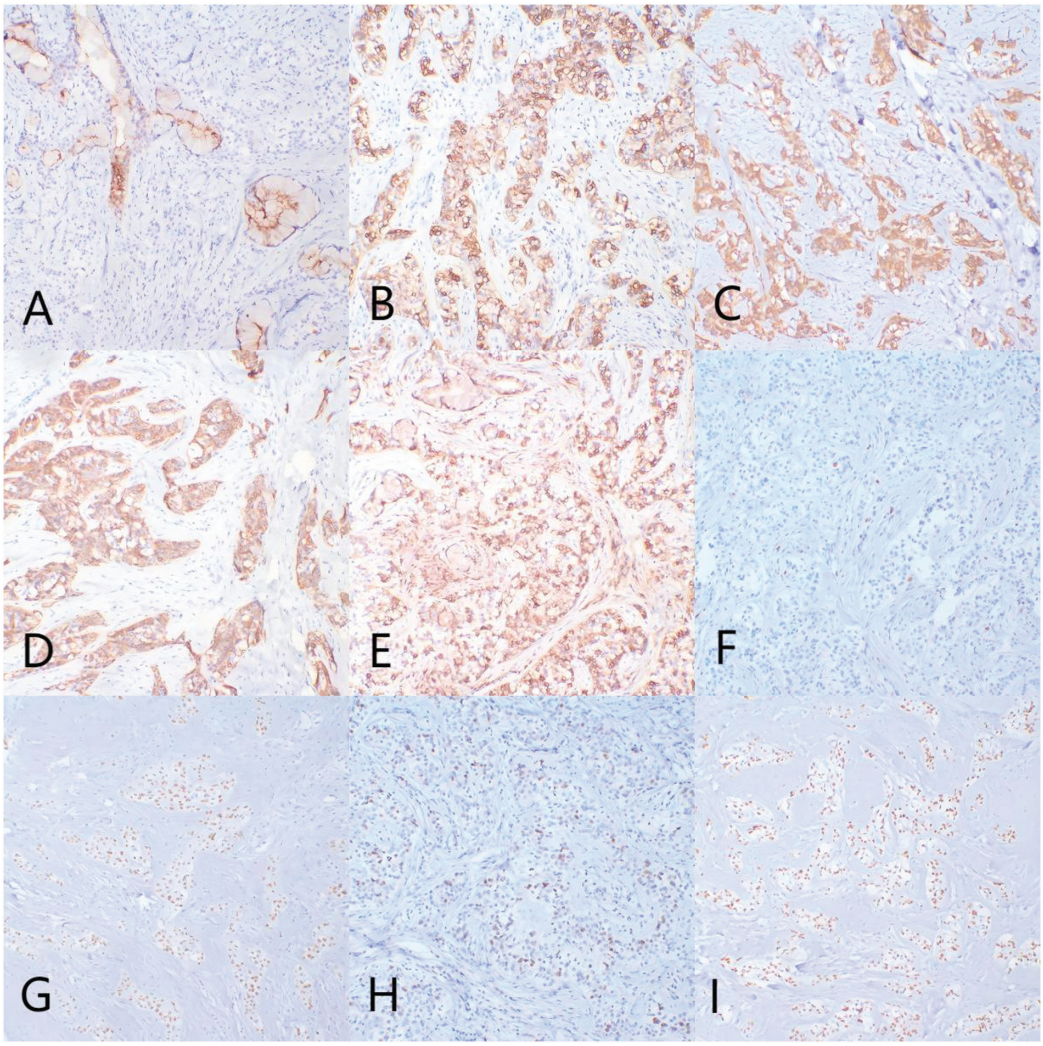

Figure 4. Immunohistochemical staining results for the tracheal tumor. (A) Carcinoembryonic antigen: Positive staining in tumor cells forming glandular structures (x100 magnification). (B) CK7: Diffuse strong positivity in tumor cells (x100 magnification). (C) CK5/6: Diffuse strong positivity in tumor cells (x100 magnification). (D) Pan-cytokeratin: Diffuse strong positivity in tumor cells (x100 magnification). (E) Epithelial membrane antigen: Diffuse strong positivity in tumor cells (x100 magnification). (F) Ki-67: Staining demonstrating a low proliferative index, with <5% positivity (x100 magnification). (G) p40: Positive staining in tumor cells (x100 magnification). (H) p63: Positive staining in tumor cells (x100 magnification). (I) p53: Positive staining in tumor cells, indicating potential genetic alterations (x100 magnification). CK, cytokeratin.

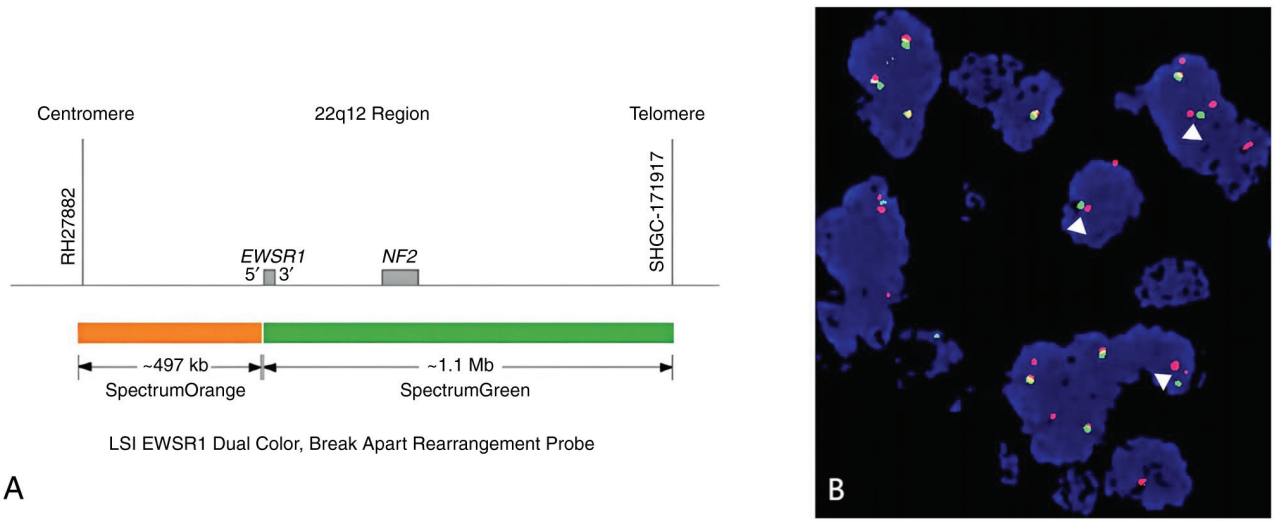

Figure 5. FISH analysis of the EWSR1 gene rearrangement. (A) Schematic representation of the dual-color break-apart probe design for the 22q12 chromosomal region. (B) FISH image showing the EWSR1 gene rearrangement, with signals indicated by white arrowheads (x1,000 magnification). LSI, locus-specific identifier; NF, normal fusion; SHGC, single hybridization gene copy; FISH, fluorescence *in situ* hybridization; EWSR1, Ewing sarcoma RNA binding protein 1.

was no evidence of recurrence and the patient remained in good health.

Discussion

HCCC is a rare, low-grade malignant epithelial tumor typically originating in the salivary glands, with pulmonary cases being particularly uncommon. The present study describes the case of a 34-year-old woman with primary tracheal HCCC, presenting as a persistent cough and dyspnea, which was successfully treated through surgical resection. The present report highlights the diagnostic challenges, and underscores the importance of comprehensive histopathological and molecular analysis in identifying this rare type of tumor. Given the rarity and low-grade malignant nature of HCCC, the necessity for prophylactic lymph node dissection currently remains uncertain. While the tumor can exhibit local invasion, its potential for lymphatic spread is not well documented due to the limited number of cases reported. In the present case, no regional lymph node metastasis was observed, supporting a more conservative approach; however, further research involving larger patient cohorts is needed to establish clear guidelines on lymph node management in HCCC.

Current knowledge of HCCC is largely derived from head and neck pathological studies, such as the study in which the cancer was first characterized by Milchgrub *et al* in 1994 (7). The initial and subsequent classifications of HCCC emphasize its unique histological features and frequent squamous differentiation, identified by markers such as p63 and 34bE12 (8). In the present case, diffuse positivity for squamous markers such as p63 and p40, combined with the absence of characteristic clear cell morphology, led to an initial misdiagnosis of squamous cell carcinoma, underscoring the risk of diagnostic pitfalls when using small biopsy samples. Major differential diagnoses included squamous cell carcinoma with clear cell changes, salivary gland-type tumors, such as low-grade mucoepidermoid carcinoma, and metastatic clear cell carcinoma of renal origin. In challenging patient cases, the EWSR1 gene rearrangement test provides valuable diagnostic confirmation of the diagnosis. Despite the positivity for p63, CK5/6 and differential keratins, the bland histological appearance of the tumor, its low mitotic index and the lack of keratinization provided evidence against a diagnosis of squamous cell carcinoma. Differentiating HCCC from low-grade mucoepidermoid carcinoma can be particularly challenging, as HCCC may exhibit occasional mucin-positive cells. In complex cases, FISH testing for mastermind-like transcriptional coactivator 2 and EWSR1 rearrangements can provide critical diagnostic support to clinicians.

FISH for EWSR1 rearrangement is a valuable diagnostic tool for HCCC. Between 87 and 91% of HCCC cases in the head and neck harbor EWSR1 rearrangements, most commonly involving a fusion with activating transcription factor 1 (ATF1). Reverse transcription-PCR and sequencing studies have shown that ~93% of HCCC cases feature an EWSR1-ATF1 fusion (9). In the present case, FISH analysis using a dual-color break-apart probe for EWSR1 confirmed the presence of EWSR1 rearrangement. Although EWSR1 rearrangement can also be observed in other types of tumors, such as Ewing sarcoma, desmoplastic small round cell tumor, clear cell sarcoma and myxoid chondrosarcoma, these tumor diagnoses were excluded based on their distinct clinicopathological characteristics.

The diagnosis and management of HCCC present unique challenges. Due to its rarity, HCCC is often underrecognized, leading to potential diagnostic delays. Preoperative biopsies may not always yield definitive results, necessitating postoperative pathological confirmation and molecular testing. While there is currently no standardized treatment protocol due to the rarity of this tumor, surgical resection with clear margins remains the mainstay of treatment. Despite its potential for local invasion and regional metastasis, HCCC generally has a favorable prognosis. Nevertheless, due to the rarity of this tumor, current knowledge is predominantly based on case reports, and there is a lack of cohort studies or long-term follow-up data to provide definitive survival rates or statistics. With only 22 cases reported worldwide, the clinical behavior of pulmonary HCCC is not yet completely understood (10). Tracheal HCCC is particularly rare, with the present case being only the fourth currently reported in the literature, to the best of our knowledge. The three previously reported cases of tracheal HCCC involved female patients aged 46 to 66 years, with varied smoking histories. Tumor sizes ranged from 1.3 to 2.5 cm when mentioned, and all were located in the trachea. Molecular testing in all cases confirmed EWSR1 gene rearrangement, with one case identifying an EWSR1:ATF1 gene fusion. Treatment strategies included laser therapy and cryotherapy in one case, while the other two patients underwent surgical resection, with one receiving additional radiation therapy and another receiving chemoradiation. Survival outcomes varied: One patient experienced no recurrence or metastasis at 12 months post-treatment, while another succumbed 6 years after the initial diagnosis. Compared with the present case of a 34-year-old female non-smoker treated with surgical resection, the absence of recurrence and favorable postoperative recovery align with previous reports (2-4). The Ki-67 index in the present case was notably low, consistent with the indolent clinical behavior observed in the patient, who remained disease-free at the last follow-up. Low proliferative indices, as indicated by Ki-67, can be associated with favorable outcomes in rare tumors, including HCCC. This pattern aligns with findings in other uncommon low-grade malignancies, such as certain types of clear cell tumor, which also demonstrate low Ki-67 levels and prolonged survival times (11). The low Ki-67 index in HCCC suggests that, despite its potential for local invasion, the growth rate of this tumor is generally slow, reinforcing the importance of complete surgical resection as a viable treatment strategy, with a favorable prognosis in similar cases.

Unlike the patients in previously reported cases, the present patient was relatively young, and the tumor presented with unusual tracheal obstruction, making the present case a rare example of tracheal involvement in HCCC. The diagnostic challenge was further compounded by the lack of prominent clear cell features, which initially suggested squamous cell carcinoma. This combination of clinical and diagnostic complexities highlighted the importance of a thorough histopathological and molecular analysis when identifying such rare cases, and underscored the need for clinical awareness of the atypical presentations of HCCC.

In conclusion, primary pulmonary HCCC is an exceptionally rare tumor with distinct pathological features. Further studies involving larger patient cohorts and extended follow-up are essential to improve the current understanding of its clinical behavior and to refine therapeutic strategies.

Acknowledgements

Not applicable.

Funding

The present study was funded by the Tianjin Medical Key Specialty Construction Project (project no. TJYXZDXK-018A) and the Tianjin Metrology Science and Technology Project (project no. 2024TJMT001).

Availability of data and materials

The data generated in the present study may be requested from the corresponding author.

Authors' contributions

WZ and ZW were responsible for study conception and design. XL performed the surgical procedure and contributed to the revision of the manuscript for important intellectual content. DS contributed to the formulation of the surgical strategy, provided insights into patient management, and assisted in the analysis and interpretation of clinical data. Additionally, DS revised the manuscript for intellectual content and accuracy. GG assisted with data acquisition and interpretation. WZ and ZW were responsible for the provision of study materials or patients, and the collection and assembly of data. Data analysis and interpretation was performed by WZ and ZW. All authors helped to write the manuscript. WZ and ZW confirm the authenticity of all the raw data. All authors have read and approved the final version of the manuscript.

Ethics approval and consent to participate

Not applicable.

Patient consent for publication

Written informed consent was obtained from the patient for publication of this case report and any accompanying images.

Competing interests

The authors declare that they have no competing interests.

References

1. WHO Classification of Tumours Editorial Board: Thoracic Tumours. In: WHO Classification of Tumours. 5th edition. Vol 5. International Agency for Research on Cancer, Lyon, 2021.
2. Doxtader EE, Shah AA, Zhang Y, Wang H, Dyhdalo KS and Farver C: Primary salivary gland-type tumors of the tracheobronchial tree diagnosed by transbronchial fine needle aspiration: Clinical and Cytomorphologic features with histopathologic correlation. Diagn Cytopathol 47: 1168-1176, 2019.
3. Gubbiotti MA, Montone K, Zhang P, Livolsi V and Baloch Z: A contemporary update on hyalinizing clear cell carcinoma: compilation of all in-house cases at our institution and a literature review spanning 2015-2020. Hum. Pathol 111: 45-51, 2021.
4. Icard B, Grider DJ, Aziz S and Rubio E: Primary tracheal hyalinizing clear cell carcinoma. Lung Cancer 125: 100-102, 2018.
5. American Joint Committee on Cancer (AJCC): AJCC Cancer Staging Manual. 8th edition. Amin MB, Greene FL, Edge SB, Byrd DR, Brookland RK, Washington MK, Gershenwald JE, Compton CC, Hess KR, Sullivan DC, *et al* (eds). Springer Cham, New York, NY, 2017.
6. Jurisic V, Radenkovic S and Konjevic G: The actual role of LDH as tumor marker, biochemical and clinical aspects. Adv Exp Med Biol 867: 115-124, 2015.
7. Milchgrub S, Gnepp DR, Vuitch F, Delgado R and Albores-Saavedra J: Hyalinizing clear cell carcinoma of salivary gland. Am J Surg Pathol 18: 74-82, 1994.
8. Weinreb I: Hyalinizing clear cell carcinoma of salivary gland: A review and update. Head Neck Pathol 7 (Suppl 1): S20-S29, 2013.
9. Thway K and Fisher C: Tumors with EWSR1-CREB1 and EWSR1-ATF1 Fusions: The current status. Am J Surg Pathol 36: e1-e11, 2012.
10. Wu YL, Wu F, Cao MF, Lan Y, Du MS, Yu ST, Wang Y, Yan XC, Bian XW and Duan GJ: Primary pulmonary hyalinizing clear cell carcinoma with fusions of both EWSR1::CREM and IRF2::NTRK3: Report of a case with an aggressive behavior. Front Oncol 13: 1175279, 2023.
11. Marković M, Jurišić V, Petrović M, Dagović A, Stanković V and Mitrović S: Appearance of ductal breast and colon carcinoma with gastrointestinal stromal tumor (GIST) in a female patient: An extremely rare case. Rom J Morphol Embryol 59: 613-617, 2018.